Cell Death and Differentiation (2015) 22, 862–874

www.nature.com/cdd

Granzyme B-induced mitochondrial ROS are required for apoptosis

G Jacquemin[1,5], D Margiotta[1,5], A Kasahara[1], EY Bassoy[1], M Walch[2], J Thiery[3], J Lieberman[4] and D Martinvalet*[,1]

Caspases and the cytotoxic lymphocyte protease granzyme B (GB) induce reactive oxygen species (ROS) formation, loss of transmembrane potential and mitochondrial outer membrane permeabilization (MOMP). Whether ROS are required for GB-mediated apoptosis and how GB induces ROS is unclear. Here, we found that GB induces cell death in an ROS-dependent manner, independently of caspases and MOMP. GB triggers ROS increase in target cell by directly attacking the mitochondria to cleave NDUFV1, NDUFS1 and NDUFS2 subunits of the NADH: ubiquinone oxidoreductase complex I inside mitochondria. This leads to mitocentric ROS production, loss of complex I and III activity, disorganization of the respiratory chain, impaired mitochondrial respiration and loss of the mitochondrial cristae junctions. Furthermore, we have also found that GB-induced mitocentric ROS are necessary for optimal apoptogenic factor release, rapid DNA fragmentation and lysosomal rupture. Interestingly, scavenging the ROS delays and reduces many of the features of GB-induced death. Consequently, GB-induced ROS significantly promote apoptosis.

Cell Death and Differentiation (2015) **22,** 862–874; doi:10.1038/cdd.2014.180; published online 31 October 2014

To induce cell death, human granzyme B (GB) activates effector caspase-3 or acts directly on key caspase substrates, such as the proapoptotic BH3 only Bcl-2 family member Bid, inhibitor of caspase-activated DNase (ICAD), poly-(ADP-ribose) polymerase-1 (PARP-1), lamin B, nuclear mitotic apparatus protein 1 (NUMA1), catalytic subunit of the DNA-dependent protein kinase (DNA-PKcs) and tubulin.[1–3] Consequently, caspase inhibitors have little effect on human GB-mediated cell death and DNA fragmentation.[2] GB causes reactive oxygen species (ROS) production, dissipation of the mitochondrial transmembrane potential ($\Delta\Psi$m) and MOMP, which leads to the release of apoptogenic factors such as cytochrome *c* (Cyt *c*), HtrA2/Omi, endonuclease G (Endo G), Smac/Diablo and apoptosis-inducing factor, from the mitochondrial intermembrane space to the cytosol.[4–11] Interestingly, cells deficient for Bid, Bax and Bak are still sensitive to human GB-induced cell death,[5,11–13] suggesting that human GB targets the mitochondria in another way that needs to be characterized. Altogether, much attention has been focused on the importance of MOMP in the execution of GB-mediated cell death, leaving unclear whether ROS production is a bystander effect or essential to the execution of GB-induced apoptosis. The mitochondrial NADH: ubiquinone oxidoreductase complex I is a key determinant in steady-state ROS production. This 1 MDa complex, composed of 44 subunits,[14] couples the transfer of two electrons from NADH to ubiquinone with the translocation of four protons to generate the $\Delta\Psi$m. The importance of ROS has been previously demonstrated for caspase-3 and granzyme A (GA) pathways through the cleavage of NDUFS1 and NDUFS3, respectively.[15–18] GA induces cell death in a Bcl-2-insensitive and caspase- and MOMP-independent manner that has all the morphological features of apoptosis.[1,16–20] As GA and GB cell death pathways are significantly different, whether ROS are also critical for GB still need to be tested. Here, we show that GB induces ROS-dependent apoptosis by directly attacking the mitochondria in a caspase-independent manner to cleave NDUFS1, NDUFS2 and NDUFV1 in complex I. Consequently, GB inhibits electron transport chain (ETC) complex I and III activities, mitochondrial ROS production is triggered and mitochondrial respiration is compromised. Interestingly, MOMP is not required for GB to cleave the mitochondrial complex I subunits and ROS production. Moreover, GB action on complex I disrupts the organization of the respiratory chain and triggers the loss of the mitochondrial cristae junctions. We also show that GB-mediated mitocentric ROS are necessary

[1]CMU, Cell Physiology and Metabolism, Faculté de Médecine, Université de Genève, Geneva, Switzerland; [2]Unité d'Anatomie, Departement de Médecine, Université de Fribourg, Fribourg, Switzerland; [3]INSERM U753, Gustave Roussy Cancer Campus, Villejuif, France and [4]Program in Cellular and Molecular Medicine, Boston Children's Hospital, Harvard Medical School, Boston, MA, USA
*Corresponding author: D Martinvalet, CMU, Cell Physiology and Metabolism, Faculty of Medicine, University of Geneva, Rue Michel-Servet 1, Geneva 1211, Switzerland. Tel: +41 22 379 5285; Fax: +41 22 379 52 60; E-mail: Denis.Martinvalet@unige.ch
[5]These authors contributed equally to this work.

Abbreviations: $\Delta\Psi$m, mitochondrial transmembrane potential; Bax, Bcl-2-associated X protein; Bcl-2, B-cell CLL/lymphoma 2; Bid, BH3-interacting domain death agonist; BNGE, blue native gel electrophoresis; Cyt c, cytochrome c; D, digitonin; Endo G, endonuclease G; ETC, electron transport chain; GA, granzyme A; GB, granzyme B; HAX-1, HCLS1-associated protein X-1; HBSS, Hank's balanced salt solution; HE, dihydroethidium; ICAD, inhibitor of caspase-activated DNase; LM, lauryl maltoside; MEF, mouse embryonic fibroblast; MnTBAP, Mn(III)tetrakis (4-benzoic acid) porphyrin; MOMP, mitochondrial outer membrane permeabilization; mtDNA, mitochondrial DNA; NAC, *N*-acetyl cysteine; NADH, nicotinamide adenine dinucleotide; NDUFA9/13, NADH dehydrogenase (ubiquinone) 1α subcomplex, 9/13; NDUFS1/2/3/7, NADH dehydrogenase (ubiquinone) Fe-S protein 1/2/3/7; NDUFV1, NADH dehydrogenase (ubiquinone) flavoprotein 1; NOX, NADPH oxidase; P, perforin; PARP, poly-(ADP-ribose) polymerase; PI, propidium iodide; PK, proteinase K; ROS, reactive oxygen species; SC, supercomplex; TPP, triphenylphosphonium; UQCRB, ubiquinol-cytochrome *c* reductase binding protein; UQCRC1/2, ubiquinol-cytochrome *c* reductase core protein 1/2; UQCRFS1, ubiquinol-cytochrome *c* reductase, Rieske iron-sulfur polypeptide 1; WB, western blot; WT, wild type

Received 27.5.14; revised 01.9.14; accepted 23.9.14; Edited by L Scorrano; published online 31.10.14

for proper apoptogenic factor release from the mitochondria to the cytosol and for the rapid DNA fragmentation, both hallmarks of apoptosis. Moreover, GB-induced ROS are necessary for lysosomal membrane rupture. Thus, our work brings a new light to the GB pathway, showing that GB-mediated mitochondrial ROS are not adventitious waste of cell death, but essential mediators of apoptosis.

Results

GB disrupts complex I by cleaving NDUFV1, NDUFS2 and NDUFS1. To test whether ROS are necessary for GB rapid induction of cell death, K562 cells were treated with a sublytic concentration of perforin (P) and GB in the presence or absence of the antioxidants Mn(III)tetrakis (4-benzoic acid) porphyrin (MnTBAP) or *N*-acetyl cysteine (NAC). MnTBAP and NAC reduced both GB-induced mitochondrial ROS production and cell death in a dose-dependent manner as detected by MitoSOX and Annexin-propidium iodide (PI) staining, respectively (Figure 1a and Supplementary Figures 1a and b). MnTBAP also inhibits GB-induced ROS increase when detected with dihydroethidium (HE) that reacts with total superoxide anion (Supplementary Figure 1c). Moreover, MnTBAP significantly protects the B-cell line 721.221 from YT-Indy human NK cell line that mainly abundantly expresses GB (Figure 1b), indicating that GB induces ROS-dependent apoptosis. The mitochondria-targeted ROS scavenger MitoQ[21] completely scavenges GB-induced ROS and inhibits cell death, suggesting that GB induces mitochondrial ROS-dependent apoptosis (Figure 1c). By 2D gel electrophoresis and mass spectrometry analysis of the mitochondria treated or not with GB or GA, we identified NDUFV1 as a putative GB target (Figure 1d). The mass spectrometry data identified eight peptides covering more than 40% of NDUFV1 protein. NDUFV1 is a 51 kDa iron-sulfur (Fe-S) cluster-containing subunit that catalyzes the initial transfer of electrons from NADH across complex I to ubiquinone, making it a good candidate target for GB-induced ROS.[22–25] GB and P treatment of K562 cells induced a dose- and time-dependent cleavage of NDUFV1 comparable to PARP-1 cleavage (Figure 1e). The caspase inhibitors z-VAD-fmk and DEVD-fmk have a partial effect, whereas the GB inhibitor Ac-IETD-CHO prevented NDUFV1 cleavage. Using CutDB and SitePrediction bioinformatics tool,[26,27] we found that GB has predicted cleavage sites for NDUFV1, NDUFS2, NDUFS1, NDUFS3, NDUFS7 and NDUFA13. Similar to NDUFV1, both NDUFS1 and NDUFS2 were cleaved in K562 cells treated with GB and P similarly to PARP-1 (Figure 1f and data not shown). GB cleavage of NDUFS1 and NDUFS2 was slightly affected by z-VAD-fmk (Supplementary Figure 1d and data not shown). The dose of z-VAD used was effective as it inhibits caspase cleavage of PARP (89 kDa fragment) and prevents caspase-3 autoprocessing from p19 to p17 (Supplementary Figure 1d). Tagged complex I subunits overexpressed in the B-cell line 721.221, or MEF localized to the mitochondria and integrated into complex I (Supplementary Figures 1e–g and data not shown). GB induced a dose- and time-dependent cleavage of tagged NDUFV1, NDUFS2 and NDUFS1 similar to PARP-1 and HAX-1[11,12] cleavage (Supplementary Figures 2a–c). GB did not cleave NDUFS3, NDUFS7 or NDUFA13 (data not shown). Tagged NDUFV1, NDUFS2 and NDUFS1 were also cleaved when 721.221 cells were incubated with YT-Indy (Figures 1g–i). Moreover, the caspase-3-uncleavable mutant of NDUFS1 (D255A-NDUFS1) was also cleaved, confirming that it is a direct GB substrate (Figure 1h). In the presence of cycloheximide that inhibits protein synthesis and *de novo* complex I production, GB and P still cleave complex I subunits, indicating that GB is acting on fully assembled complex I (Supplementary Figure 2d).[28–30] NDUFS3 and NDUFA9 complex I subunits not cleaved by GB were still present long after the cells had died following 4 h of GB treatment (Supplementary Figure 2e). Altogether, GB, independently of caspases, cleaves NDUFV1, NDUFS2 and NDUFS1 in cells undergoing killer cell attack.

GB cleaves recombinant NDUFV1, NDUFS1 and NDUFS2 and cleaves these proteins in intact mitochondria. CutDB predicts that GB will cleave NDUFV1 after D118 and D338/340 (Supplementary Figure 3a), NDUFS1 after D364 (Supplementary Figure 3b) and NDUFS2 after D317 (Supplementary Figure 4). These cleavage site sequences are conserved between mice and humans. The cleavage fragment sizes corresponded roughly to predicted cleavage sites. The D–A mutations at the predicted cleavage sites protect from GB, confirming that NDUFV1, NDUFS1 and NDUFS2 are direct GB substrates. In isolated intact mitochondria, GB cleaved all three of these complex I subunits, but not NDUFS3 or NDUFA13, within 1 min (Figure 2a). The cleavage of the subunits was inhibited by valinomycin-mediated mitochondrial ΔΨm loss, suggesting that GB needs an intact ΔΨm to reach its substrates inside the mitochondrial matrix.

GB-induced ROS are mediated by complex I subunits cleavage, are independent of caspase activation and potentiate cell death. Overexpression of GB-uncleavable forms of complex I subunits (triple mutant) significantly reduced and slowed down GB-mediated ROS production, compared with cells overexpressing the wild-type (WT) substrates (triple WT) (Figures 2b–d). Thus, mitochondrial complex I proteolysis is a major contributor to ROS generation in this pathway. The presence of endogenous NDUFV1, NDUFS2 and NDUFS1 might account for some residual ROS production. However, the silencing of these endogenous subunits in triple mutant cells triggers spontaneous ROS production (data not shown). Overexpression of these uncleavable mutant proteins also significantly inhibited and slowed down GB-mediated cell death (Figures 2e and f). GB-mediated ROS production and cell death in triple WT and triple mutant cells was caspase-independent (Figures 2g and h). Thus, GB induces mitocentric ROS by cleaving NDUFV1, NDUFS2 and NDUFS1 independently of caspases to promote apoptosis.

GB cleaves complex I subunits independently of MOMP. Purified mitochondria were treated with GB in the presence or absence of S100 cytosolic fraction as a source of Bid, and

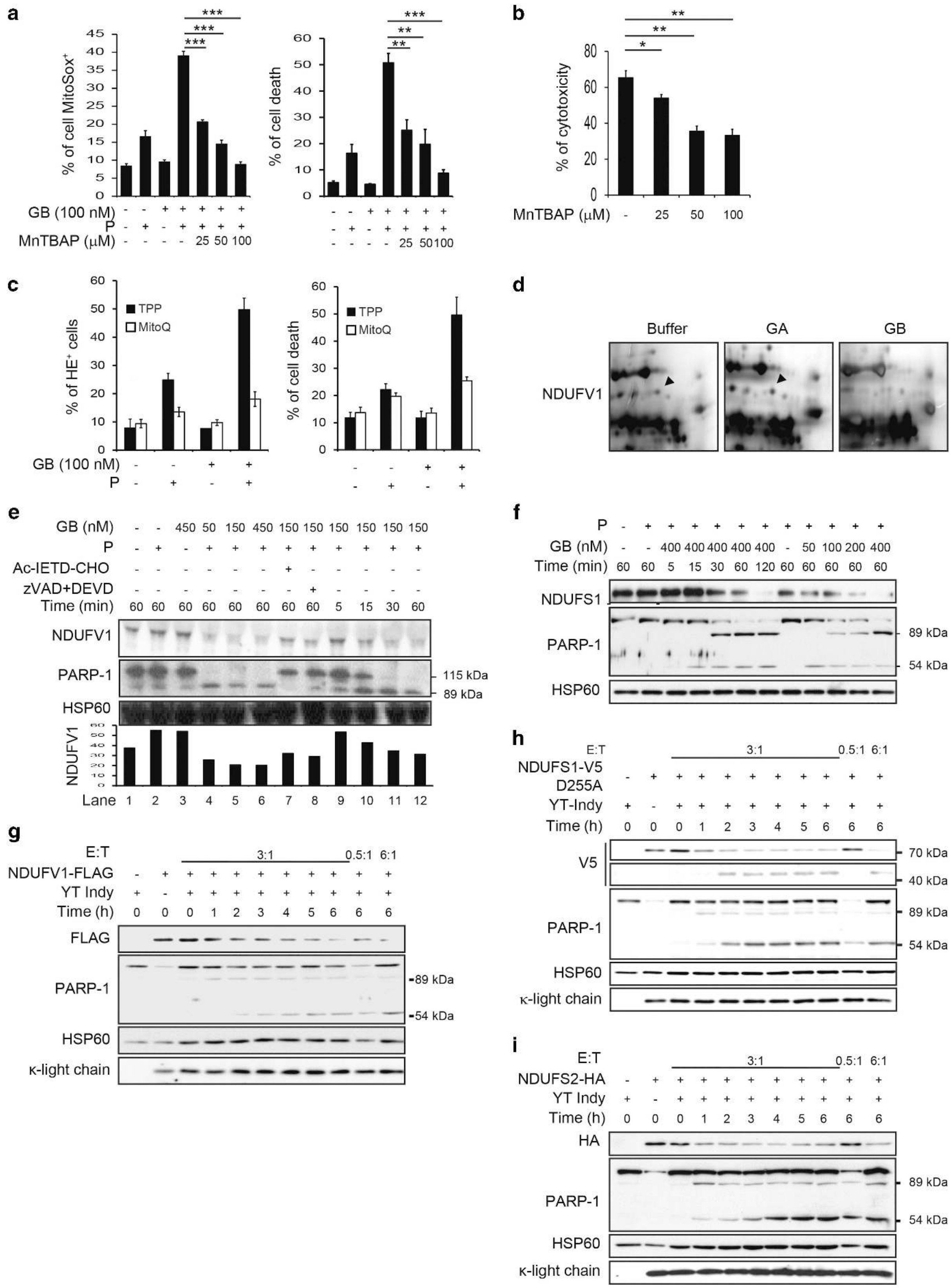
a
% of cell MitoSox+
% of cell death
GB (100 nM)
P
MnTBAP (μM)
25 50 100
b
% of cytotoxicity
MnTBAP (μM)
25 50 100
c
% of HE+ cells
% of cell death
TPP
MitoQ
GB (100 nM)
P
d
Buffer
GA
GB
NDUFV1
e
GB (nM)
P
Ac-IETD-CHO
zVAD+DEVD
Time (min)
NDUFV1
PARP-1
HSP60
115 kDa
89 kDa
Lane
f
P
GB (nM)
Time (min)
NDUFS1
PARP-1
HSP60
89 kDa
54 kDa
g
E:T
3:1
0.5:1
6:1
NDUFV1-FLAG
YT Indy
Time (h)
FLAG
PARP-1
HSP60
κ-light chain
h
NDUFS1-V5
D255A
YT-Indy
V5
70 kDa
40 kDa
i
NDUFS2-HA
HA

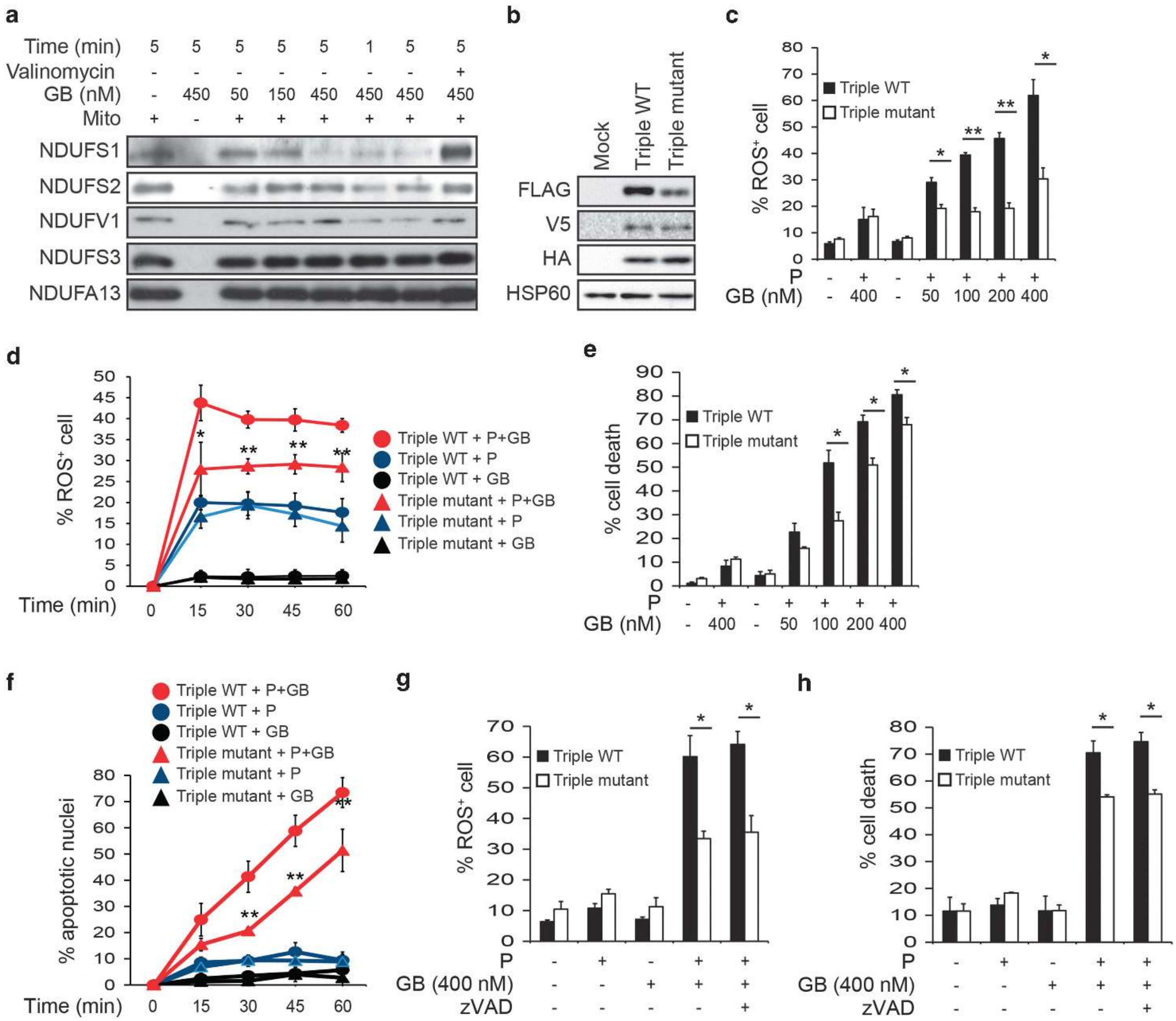

Figure 2 Overexpression of GB-uncleavable NDUFS1, NDUFS2 and NDUFV1 protects against GB-induced ROS production and cell death. (**a**) Purified intact mouse liver mitochondria, pretreated or not with valinomycin, were incubated with GB and probed for complex I subunits. (**b**) Expression of WT (triple WT) and GB-uncleavable NDUFV1-3xFLAG, NDUFS2-HA and NDUFS1-V5 (triple mutant) proteins in untransfected or transfected K562 cells. (**c**–**h**) Transfected K562 cells were treated with P ± GB as indicated and assessed for mitochondrial ROS by MitoSOX staining and flow cytometry (**c**, **d** and **g**) and for cell death by Annexin V-PI staining and flow cytometry (**e** and **h**) or counting of apoptotic nuclei stained by Hoechst 33342 (**f**, mean of at least 300 nuclei per conditions, from three independent experiments). P+GB (red lines), P alone (blue lines), GB alone (black lines), triple WT (circles) and triple mutant (triangles). In (**g** and **h**), cells were pretreated or not with z-VAD-fmk to inhibit caspases. Mean ± S.E.M. of at least three independent experiments is shown, *$P<0.05$ and **$P<0.01$

Figure 1 GB cleaves complex I subunits NDUFS1, NDUFV1 and NDUFS2. (**a**) K562 cells pretreated or not for 1 h with MnTBAP were treated with P ± GB as indicated. ROS (MitoSOX+, left panel) and cell death (Annexin V-PI, right panel) were monitored at 10 and 45 min, respectively. (**b**) The 721.221 target cells preincubated or not with MnTBAP for 1 h were mixed with YT-Indy effector cells expressing only GB at an E / T ratio of 12 : 1. Target cell killing was monitored by calcein release assay. (**c**) K562 cells preincubated for 1 h with 20 μM of the mitochondria-targeted antioxidant MitoQ or decyl-TPP as a control were treated with P ± GB as indicated. ROS (dihydroethidium positive (HE+), left panel) and cell death (Annexin V-PI, right panel) were monitored after 10 and 45 min, respectively. (**a**–**c**) Mean ± S.E.M. of at least three independent experiments, **$P<0.01$ and ***$P<0.001$. (**d**) Close-up of 2D isoelectric focusing (IEF) SDS-PAGE gels of purified intact mouse liver mitochondria treated or not with GB or GA. The spot indicated by the arrow was identified as NDUFV1 by mass spectrometry. (**e** and **f**) K562 cells, treated with P ± GB as indicated, were analyzed by immunoblot probed for NDUFV1 (**e**) and NDUFS1 (**f**), PARP-1 and Hsp60. Some cells were pretreated for 30 min with the caspase inhibitors Z-Val-Ala-Asp-fluoromethylketone (z-VAD-fmk) and Z-Asp-Glu-Val-Asp-fluoromethylketone (DEVD-fmk) or with the GB-specific inhibitor Ac-Ile-Glu-Thr-Asp-CHO (Ac-IETD-CHO). NDUFV1 bands quantification in the lower panel (**e**) was measured with the ImageJ software (National Institutes of Health, Bethesda, MD, USA). (**g**–**i**) The 721.221 target cells, transfected with tagged NDUFV1 (**g**), caspase-3-uncleavable D255A-NDUFS1 (**h**) or NDUFS2 (**i**) were treated with YT-Indy NK cells at indicated effector/target (E/T) ratios and probed for the ectopically expressed complex I proteins using anti-tag antibodies. Experiments in (**e**–**i**) were repeated at least three times with similar results apoptogenic factors release was followed to assess MOMP.[4,6–10] GB induced Cyt *c* and Endo G release only in the presence of S100 (Figure 3a), whereas cleavage of NDUFS1 occurred in the absence of S100 (Figure 3a). Interestingly, NDUFS1 cleavage was increased in the presence of S100, most likely as the result of the combined action of GB and caspase-3. Moreover, GB still induces ROS and cell death in Bax- and Bak-deficient mouse embryonic fibroblasts (MEFs),[31] although to a lower extent compared with the WT counterpart (Figures 3b–d). Note that the level of GB-induced ROS corresponds to the extent of cell death following GB treatment of $Bax^{-/-}$ and $Bak^{-/-}$ MEF. The higher level of ROS observed in WT MEF could be because of the combined action of GB and caspase-3 on complex I subunits cleavage as observed in Figure 3a. GB cleaved tagged NDUFV1, NDUFS2 and NDUFS1 similarly in WT and $Bax^{-/-}$/$Bak^{-/-}$ MEFs (Figures 3e and f). Thus, GB induces complex I subunit cleavage and ROS independently of MOMP. Therefore, GB does not need the opening of the mitochondrial outer membrane generated by the MOMP to enter the mitochondria and to cleave complex I subunits.

GB-induced ROS are necessary for apoptogenic factor release and oligonucleosomal DNA fragmentation. ROS have been shown to enhance apoptogenic factor release.[32–34] Interestingly, although NAC did not alter GB-induced Bid cleavage, NAC reduced and delayed the release of Cyt *c*, Endo G and Smac triggered by GB (Figures 4a–c). Moreover, neither NAC nor MitoQ prevents GB cleavage of complex I subunits (Supplementary Figure 5a). Similarly, triple mutant cells experienced GB-mediated Bid cleavage while they are resistant to GB-induced apoptogenic factor release (Figures 4d–f). We obtained similar results when Cyt *c* distribution was assessed by immune staining following GB and P treatment of triple mutant K562 cells (Figure 4g). Thus, GB-mediated mitocentric ROS also promote the release of apoptogenic factors.

Moreover, the well-characterized GB-mediated DNA fragmentation[35,36] was reduced and delayed by NAC treatment (Figures 4h and i). In a similar manner, triple mutant cells were also resistant to GB-induced DNA fragmentation (Figure 4j). Neither NAC nor overexpression of GB-uncleavable complex I subunits inhibits GB-induced ICAD cleavage (data not shown). Altogether, this indicates that GB-mediated mitocentric ROS are also required for oligonucleosomal DNA fragmentation.

GB-induced ROS are necessary for lysosomal membrane rupture. Mitochondrial ROS have been implicated in lysosomal disruption in tumor necrosis factor-mediated cell death.[35] Lysosomal green staining began to decline in

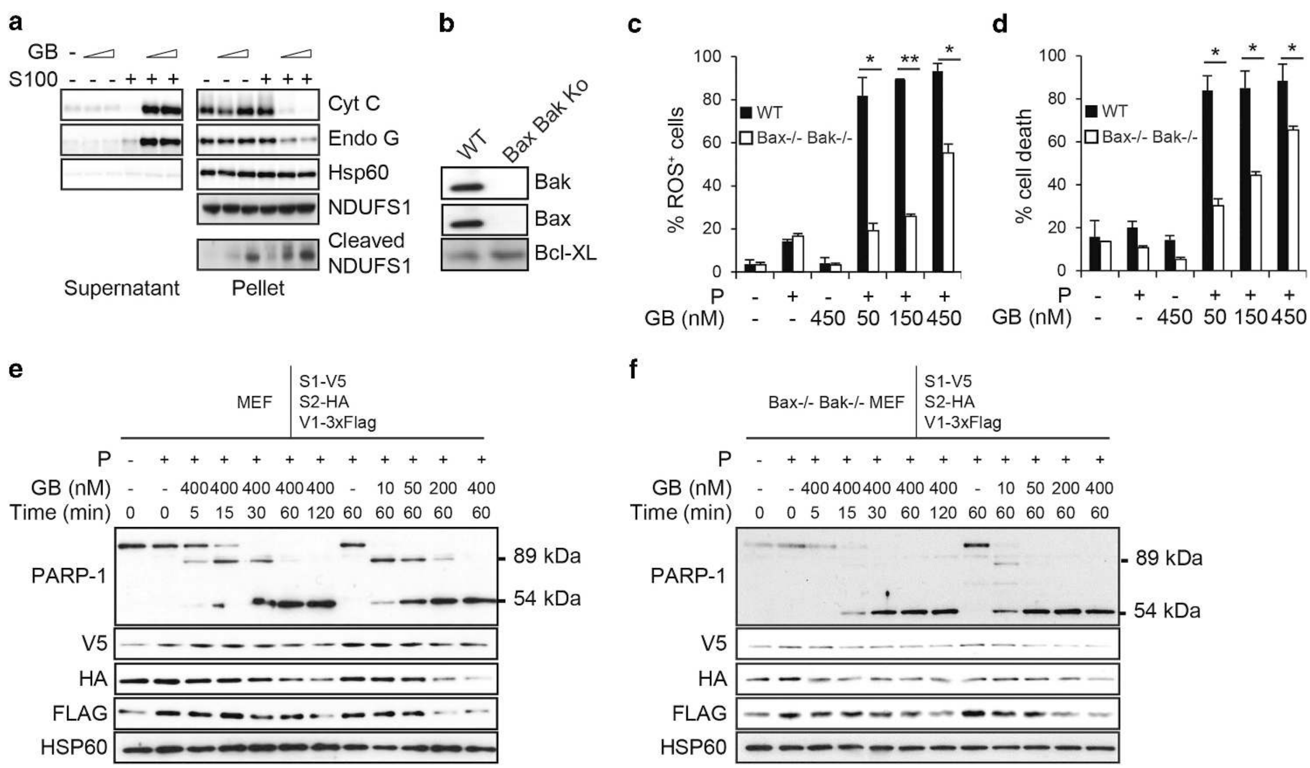

Figure 3 GB cleaves NDUFS1, NDUFV1 and NDUFS2 independently of MOMP. (**a**) Cyt *c* and Endo G release and NDUFS1 cleavage were assessed by immunoblot of supernatants and mitochondrial pellets from purified intact mouse liver mitochondria treated with 50 and 450 nM of GB in the presence or absence of S100 cytosolic fraction. Hsp60 was probed as a loading control protein that is not released. (**b**) $Bax^{-/-}Bak^{-/-}$ MEF do not express Bax or Bak as assessed by immunoblot. (**c** and **d**) ROS production (**c**) and cell death (**d**) assessed by MitoSOX and Annexin V-PI staining, respectively, in WT and $Bax^{-/-}Bak^{-/-}$ MEFs treated with GB and P for 1 h. Mean ± S.E.M. of three independent experiments is shown, $*P<0.05$ and $**P<0.01$. (**e** and **f**) WT (**e**) and $Bax^{-/-}Bak^{-/-}$ (**f**) MEFs overexpressing NDUFS1-V5, NDUFV1-3xFLAG and NDUFS2-HA were treated with GB and P as indicated and probed for NDUFS1, NDUFV1 and NDUFS2 using anti-tag antibodies. PARP-1 was probed as a control for GB activity and Hsp60 is a loading control. Blots are representative of at least three independent experiments

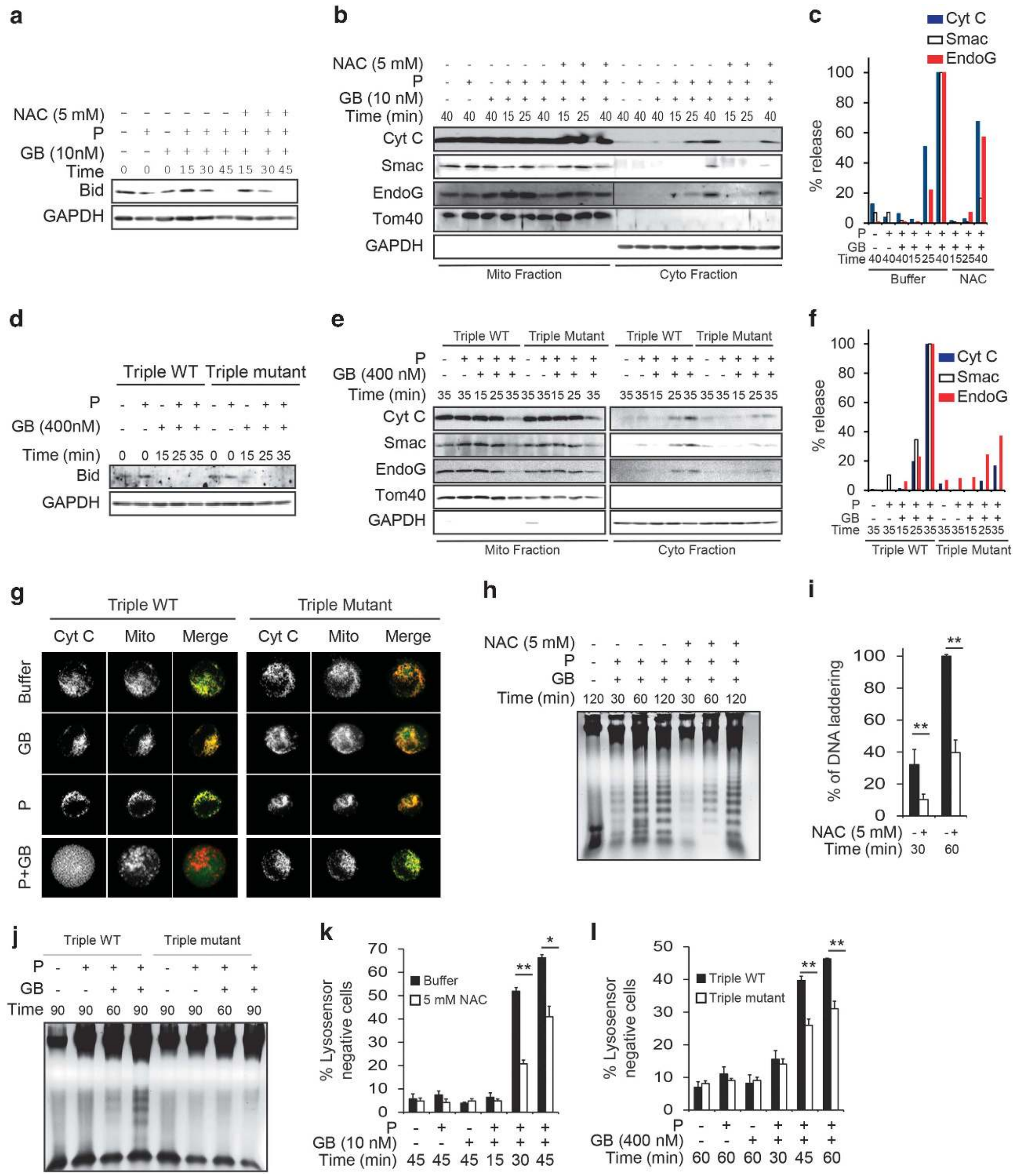

Figure 4 GB-induced ROS are required for proper apoptogenic factor release, DNA laddering and lysosomal membrane permeabilization. (**a**) Total cell lysate, (**b**) cytosolic (cyto) and mitochondrial (mito) fractions of U937 cells treated or not with P and GB, with or without NAC pretreatment were analyzed by WB for Bid cleavage and the release of Cyt *c*, Smac and Endo G from the mitochondria. Tom40 and GAPDH were probed as loading controls and to verify proper fractionation. (**c**) Quantification of the percentage of Cyt *c*, Endo G and Smac release from panel b. (**d** and **e**) K562 stably expressing WT (triple WT) or GB-uncleavable (triple mutant) NDUFV1, NDUFS1 and NDUFS2 were treated as in (**a**) to assess Bid cleavage or as in (**b**) for the release of the apoptogenic factors. (**f**) Quantification of the percentage of Cyt *c*, Endo G and Smac release from panel e. (**g**) Immunostaining for Cyt *c* of Mitotracker deep red-loaded K562 triple WT and triple mutant treated or not with GB and P for 30 min. (**h** and **i**) DNA from U937 cells, treated as in (**a**), was analyzed by agarose gel electrophoresis (and the % of DNA that migrated below 3 kb was quantified. (**h**) A representative gel and (**i**) the mean ± S.E.M. of three independent experiments. $^{**}P<0.01$. (**j**) K562 triple WT or triple mutant cells were treated and analyzed as in (**h**). A representative gel of three independent experiments is shown. (**k**) U937 cells treated as indicated with or without 5 mM NAC were stained with a Lysosensor, which only fluoresces in lysosomes that maintain acidic pH. Mean ± S.E.M. of three independent experiments. $^{*}P<0.05$ and $^{**}P<0.01$. (**l**) K562 cells overexpressing triple WT or triple mutant complex I subunits were treated and analyzed as in (**k**)

U937 cells within 30 min of GB+P treatment, as an indication of pH rises in compromised lysosomes, suggesting that lysosomal permeabilization is a feature of GB-mediated death (Figure 4k and Supplementary Figure 5b). The loss of lysosensor green staining was significantly inhibited by NAC. Moreover, overexpression of GB-uncleavable complex I subunits reduced lysosomal membrane permeabilization, suggesting that GB-induced mitocentric ROS are also necessary for this late event of apoptosis (Figure 4l and Supplementary Figure 5c).

GB-induced ROS requires a functional respiratory chain. It has been proposed that GB induces ROS, independently of mitochondria, by a caspase-dependent activation of the NADPH oxidases (NOX).[36] However, here z-VAD-fmk had no significant effect on GB-induced ROS production and cell death, and overexpression of the uncleavable complex I subunits markedly reduced ROS generation by GB (Figures 2c, d and g). The ρ^0 K562 cells that have a significant loss of mitochondrial DNA (mtDNA), no respiration and no complexes I and III (Figure 5a)[37] are completely resistant to GB-induced ROS and cell death (Figures 5b and c). Interestingly, GB still induced ROS and cell death in *NOX1*$^{-/-}$ or *NOX4*$^{-/-}$ MEFs (Figures 5d and e). As MEF does not express NOX1 and as GB induces the same level of ROS from the NOX1 KO and the NOX4 KO, we conclude that in our system the NOX contribution in GB-induced ROS and cell death is marginal relative to the mitochondrial contribution.

GB lacks a mitochondrial targeting sequence. Furthermore, cleavage of NDUFV1, NDUFS2 and NDUFS1 was MOMP-independent, suggesting that permeabilization of the outer membrane is not needed. We verified that GB enters the mitochondria by flow cytometry and western blot (WB) analysis of isolated mitochondria incubated with Alexa Fluor-647-labeled or -unlabeled GB followed by gentle proteinase K (PK) treatment to remove externally bound proteins. GB mitochondrial import was inhibited by valinomycin (Figures 5f and g). Valinomycin, which also disrupted the $\Delta\Psi$m of intact cells (Figure 5h) without altering P-mediated GB uptake into cells (Figure 5i), inhibited GB-induced ROS and cell death (Figures 5j and k). Taken together, these results show that GB requires a functional respiratory chain and intact transmembrane potential to enter the mitochondria and induce ROS-dependent cell death.

GB disrupts complex I and III activities. GB treatment rapidly reduced both the glutamate/malate- and succinate-dependent respiration of isolated mitochondria with kinetics similar to complex I cleavage (Figures 6a and b). Interestingly, when purified intact mitochondria were treated with GB and respiratory complexes were analyzed by blue native gel electrophoresis (BNGE),[38,39] GB induced a dose-dependent inhibition of complex I activity that was significant within 1 min as monitored by in-gel activity assay (Figure 6c). Unexpectedly, GB also rapidly inhibited complex III activity, whereas the activities of complexes IV and V were unaffected. Using spectrophotometric assay of mitochondria treated with GB, we confirmed that GB alters complex I and III activities, although complex IV function was untouched (Supplementary Figures 6a, c and d). Moreover, GB also had a mild effect on complex II activity (Supplementary Figure 6b). Despite the change in complex III function, GB did not cleave the complex III subunits UQCRC1, UQCRC2 and UQCRFS1, whereas mild effect was seen on UQCRB at the highest dose of GB (Figure 6d). Thus, GB rapidly inhibits complex I, II and III activity and reduces mitochondrial respiration.

GB alters the organization of the mitochondrial respiratory chain. Mitochondrial ETC complexes organize into supercomplexes (SCs) that channel electrons in response to changes in substrate availability.[28] The alteration in complex III activity we measured might be because of changes in SC formation caused by GB cleavage of complex I subunits. In lauryl maltoside (LM)-solubilized mitochondria, which preserves monomeric ETC complexes but disrupts SCs, GB reduced NDUFV1, NDUFS2 and NDUFS1, but had no effect on the complex III proteins UQCRC1, UQCR2 or UQCRS1 (Figure 6e). In digitonin (D)-solubilized mitochondria, which preserved both monomeric complexes and SCs, I+III$_2$ SC formation was greatly enhanced by GB treatment, which was more evident when probing for unaffected NDUFA13 and NDUFS3 (Figure 6g). We did not observe SC I+III2+IV probably because the mitochondria were purified from C57B6 mice that are deficient for Cox7a2l (Cyt *c* oxidase subunit VIIa polypeptide 2 like) and therefore cannot have III+IV association (Supplementary Figure 6e).[28] GB induced a significant loss in monomeric complex I and III activities, as shown previously (Figures 6c and f). In D-solubilized samples, complex I and III activities of SC I+III$_2$ were not significantly changed by GB, even though much more SC was formed after GB treatment, indicating that the specific activity of these complexes was reduced by GB treatment. Thus, GB alters mitochondrial respiratory chain organization by tilting the balance from monomeric complexes to an accumulation of SC I+III$_2$.

GB triggers loss of mitochondrial cristae junctions. Cristae morphology is a critical determinant of ETC organization and respiratory efficiency.[40] We therefore examined whether GB treatment might also affect the shape of cristae. By electron microscopy, we observed that in GB-treated mitochondria many of the cristae appeared to have lost their junction (Figures 6h and i). A better appreciation and the functional significance of GB-induced cristae disorganization will require further studies. Thus, GB has a profound effect on mitochondrial respiration, respiratory complex activity and mitochondrial morphology.

Discussion

Here we show for the first time that GB directly cleaves NDUFV1, NDUFS2 and NDUFS1 in ETC complex I, independently of caspases, to trigger mitocentric ROS-dependent apoptosis. GB-mediated cleavage of complex I subunits not only generates ROS but also has a profound effect on mitochondrial function. GB alters complex I, II and III function and disrupts mitochondrial respiration of metabolites that feed into either complex I or complex II, disrupts ETC supramolecular organization and causes cristae to detach. The generation of mitochondrial ROS in the form of superoxide, the species produced by complex I dysfunction,[41] was previously shown to be necessary for killer lymphocyte-mediated death since superoxide scavengers virtually completely inhibit death.[17,42] Here we further show that GB-mediated mitocentric ROS are necessary for optimal apoptogenic factor release, pointing out that factor release need two independent steps, (1) the permeabilization of the mitochondrial outer

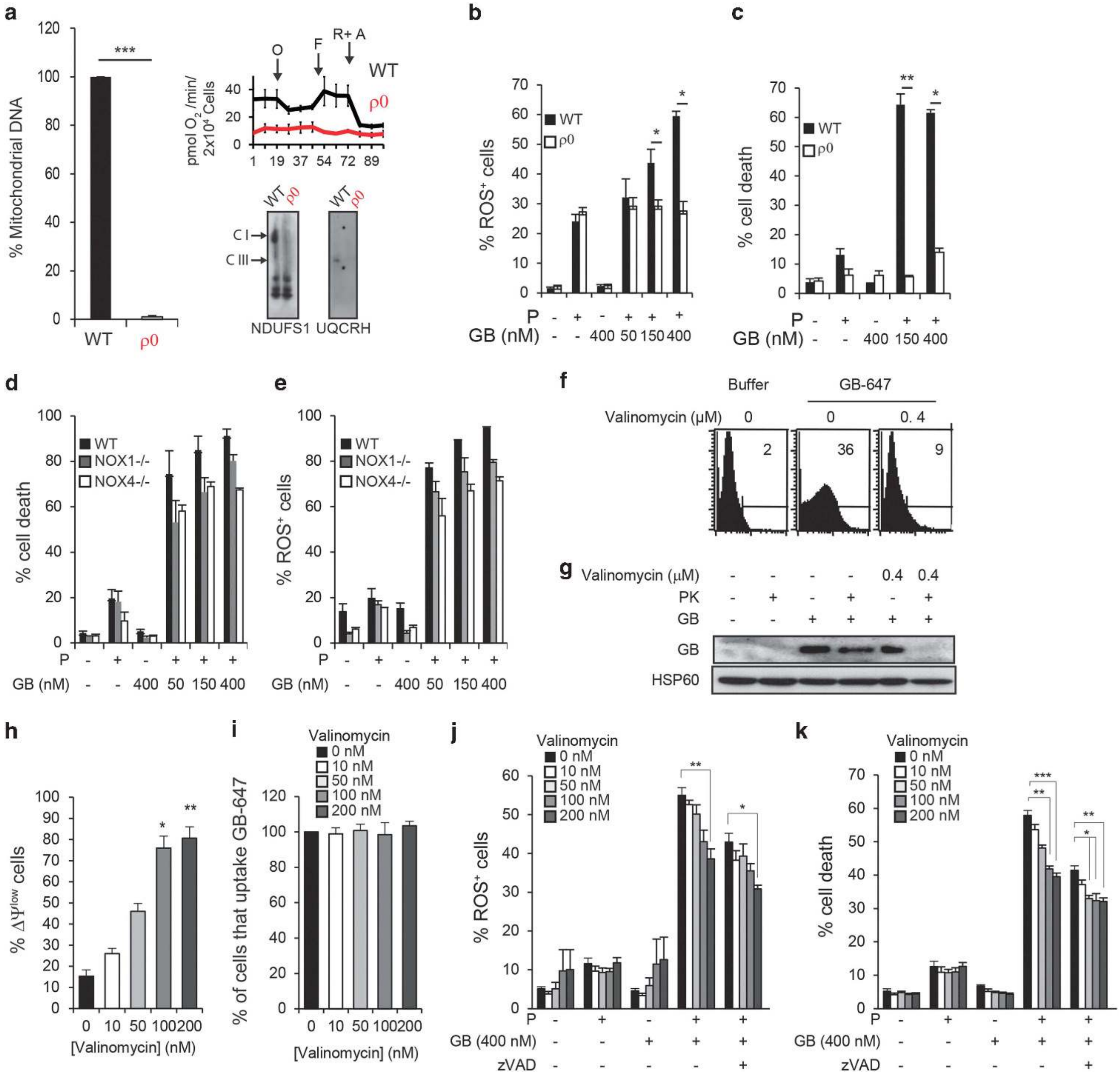

Figure 5 GB-induced ROS generation and cell death require mitochondrial respiration. (**a**) Quantification of mitochondrial DNA in WT and ρ^0 K562 cells as measured by qPCR amplification of representative genes (left panel). Oxygen consumption rate of WT and ρ^0 K562 cells assessed by seahorse measurement (top right panel) (O, oligomycin; F, FCCP; R, rotenone; A, antimycin). Analysis of complexes I and III from WT and ρ^0 K562 cells by blue native gel and WB (bottom right panel). There is a complete loss of mtDNA and complexes I and III in ρ^0 K562 cells and they do not respire. (**b** and **c**) ρ^0 K562 cells are highly resistant to GB-induced ROS production (**b**), assessed by MitoSOX staining, and cell death (**c**), assessed by Annexin V-PI staining. (**d** and **e**) WT, NOX1$^{-/-}$ and NOX4$^{-/-}$ MEFs were treated with P+GB and analyzed as above for ROS production (**d**) and cell death (**e**). (**f**) Purified intact mouse liver mitochondria treated or not with valinomycin were incubated with Alexa-647 GB before partial treatment with PK to remove externally bound proteins and analyzed by FACS. (**g**) Same as in (**f**) using unlabeled GB and analyzed by immunoblot. (**h**–**k**) Although valinomycin treatment of K562 cells depolarizes mitochondria (**h**), it has no effect on GB uptake into cells assessed by flow cytometry (**i**). Valinomycin inhibits GB-induced ROS (**j**) and cell death (**k**) in a dose-dependent manner, even in the presence of the pancaspase inhibitor z-VAD. The color code for valinomycin concentrations is as in (**h**). All graphs show mean ± S.E.M. of at least four independent experiments. *$P<0.05$, **$P<0.01$ and ***$P<0.001$

membrane following GB cleavage of Bid, which trigger Bax/Bak oligomerization and MOMP, (2) ROS that untether the apoptogenic factors within the intermembrane space for their release into the cytosol. Mitocentric ROS are also required for proper oligonucleosomal DNA fragmentation. This is in agreement with the fact that Endo G release is ROS-dependent, knowing that Endo G synergize with CAD for DNA fragmentation. Interestingly, NAC does not prevent GB-mediated ICAD cleavage (data not shown). We have reported that ROS were necessary for the SET complex containing GA-activated DNAses (three prime repair exonuclease 1 and nm23-H1) nuclear translocation upon

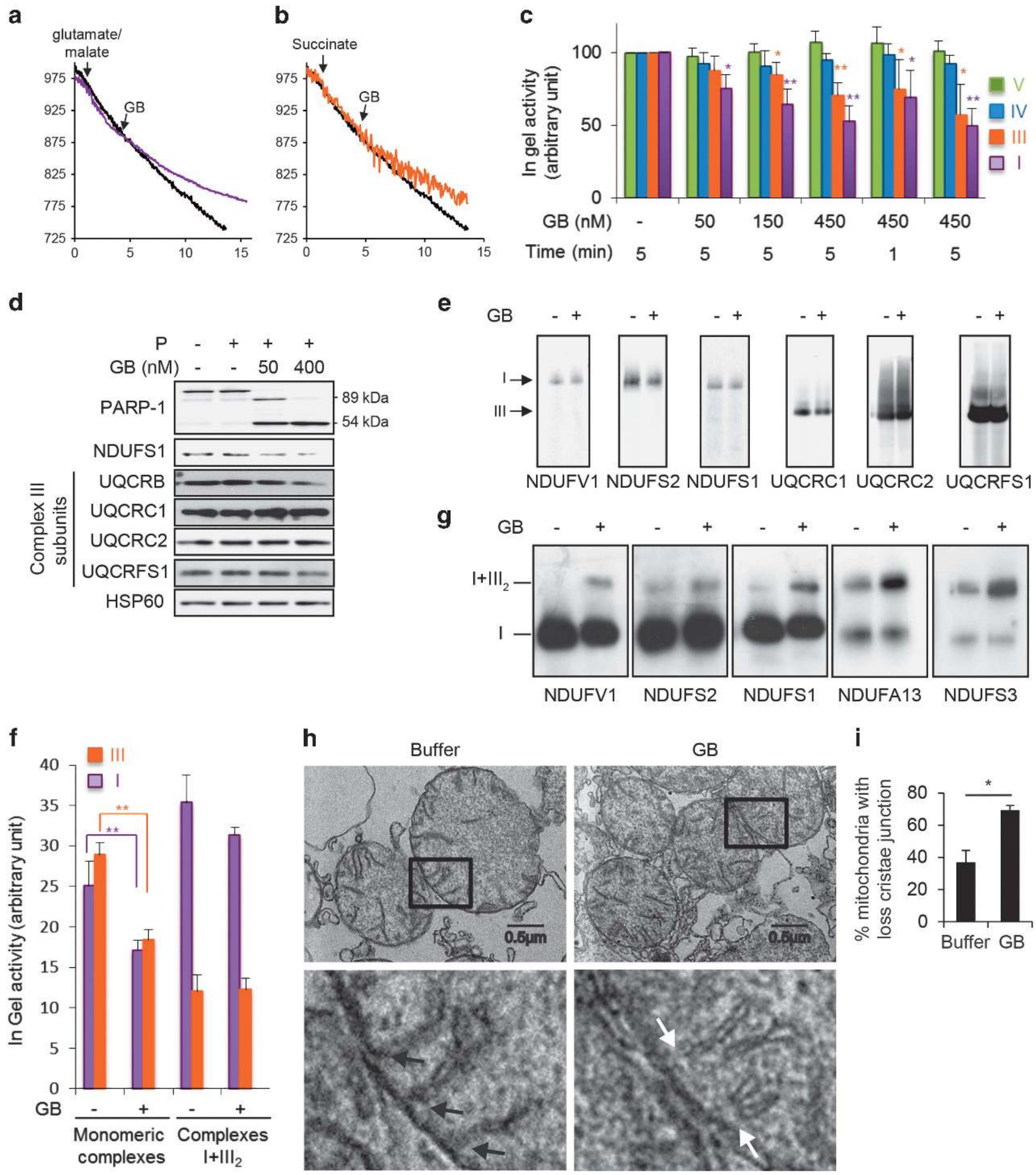

Figure 6 GB disrupts complex I and III activity. (**a** and **b**) Purified mouse liver mitochondria in respiration buffer were stimulated with glutamate/malate (**a**) or succinate (**b**) and O_2 consumption was measured using a Clark electrode. Within 1 min of GB treatment, respiration of GB-treated mitochondria (purple and orange lines) was reduced compared with untreated mitochondria (black lines). Data are representative of at least three independent experiments. (**c**) Purified mitochondria were treated with GB as indicated. Monomeric mitochondrial respiratory complexes were solubilized using LM and resolved by BNGE before measuring in-gel ETC complex activities. Mean ± S.E.M. of three independent experiments is shown. $^*P<0.05$ and $^{**}P<0.01$. (**d**) The 721.221 cells, treated with GB and P, were probed for complex III proteins. The GB substrates NDUFS1 and PARP-1 were probed as positive controls and Hsp60 as a loading control. Blots are representative of at least three independent experiments. (**e–g**) Isolated liver mitochondria treated with 450 nM GB for 5 min were solubilized with LM to resolve monomeric complexes (**e**) or D to preserve SCs (**g**) and analyzed by BNGE and immunoblot. Blots are representative of at least four independent experiments. (**f**) Complex I and III in-gel activity was monitored in monomeric complexes after LM solubilization and I+III2 SC after D solubilization. Shown are mean ± S.E.M. of four independent experiments. $^{**}P<0.01$. (**h**) Representative electron micrographs after C57B6 mouse liver mitochondria were treated with buffer or GB. GB treatment triggers loss of mitochondrial cristae junctions. White arrows indicate detached cristae, whereas black arrows show attached cristae. (**i**) The proportion of mitochondria with detached cristae was quantified and represented as the mean ± S.E.M. of three independent experiments is shown. $^*P<0.05$ and $^{**}P<0.01$

GA-induced cell death.[16,17] It is possible that in a similar manner, ROS are required for the nuclear translocation of CAD and Endo G. Additional work will be required to test this possibility. Moreover, ROS damage the integrity of the lysosomal compartment, probably following redox modification of proteins and lipids of this compartment.

GA, caspase-3 and now GB proteolyzed subunits of complex I to induced ROS-dependent apoptosis,[15,16] making complex I a point of crosstalk for three distinct cell death pathways. We have recently found that granzymes are delivered into bacteria to cleave multiple components of bacterial complex I to generate ROS-dependent bacteria death.[43] Thus, complex I disruption and ROS production are conserved biochemical mechanisms important for executing programmed cell death in two evolutionary kingdoms.

Our results indicate that GB must enter the mitochondrial matrix to cleave its substrates in the matrix-protruding arm of complex I. How does GB (or for that matter GA and caspase-3), which lack mitochondrial targeting sequences, get into the mitochondrial matrix is still unknown. GB mitochondrial entry does not require MOMP, but does require an intact ΔΨm. As MOMP dissipates the ΔΨm, GB may only enter the mitochondria that have not undergone MOMP or before MOMP dissipates the ΔΨm.

GB-induced ROS required mitochondrial electron flow as ρ^0 K562 cells were resistant to both GB-induced ROS and cell death. This result and our finding that ROS generation is caspase-independent differ from a previous work,[36] which implicated NOX oxidases in ROS generation by GB. However, we found that GB generation of ROS and cell death were not significantly reduced in *NOX1*$^{-/-}$ or *NOX4*$^{-/-}$ MEFs, suggesting that mitochondria rather than NOX proteins are the primary source of ROS in GB cell death pathway.

Based on the crystal structure of *Thermus thermophilus* complex I, mammalian NDUFV1, NDUFV2 and NDUFS1 are predicted to be localized at the tip of the matrix-protruding arm of complex I, exposed to solvent[30,44] and hence be accessible to GB. We found that complex I within SC I+III_2 is also altered by GB. This is consistent not only with the function of those subunits in forming the electron entry site but also with the topology of SC I+III_2 as dimeric complex III associates with the membrane segment of complex I, leaving the matrix-protruding arm free.[45,46]

Cleavage of NDUFS1, NDUFS2 and NDUFV1 would be expected to disrupt complex I function and favor a leakage of the electrons to produce ROS. GB unexpectedly inhibited complex III activity and succinate-dependent respiration. We did not observe cleavage of tested complex III subunits, except a mild effect on UQCRB. It is possible that GB also acts on other complex III subunits we did not evaluate. Moreover, GB has a mild effect on complex II activity. This plus the increased SC I+III_2 formation may help explain why GB compromises respiration of the complex II substrate succinate. Taken together, it appears that GB hits multiple site of the respiratory chain at the level of complex I, II and complex III that will alter the electron flow and favor the formation of mitocentric ROS.

In intact complex I, the Fe-S centers and their associated electrons are buried in the protein part of the subunits to shield them from ambient O_2. GB, by cleaving these subunits close to their Fe-S centers (Supplementary Figures 3 and 4), may expose electrons within the Fe-S centers to ambient oxygen allowing their direct reaction to form superoxide. Reverse electron transport accounts for most $O_2^{\cdot-}$ production by complex I under basal conditions in a process that involves reduced ubiquinone.[47,48] NDUFS2 establishes a groove with NDUFS7 to form the ubiquinone binding site.[23–25] GB cleavage of NDUFS2 may alter the ubiquinone binding site to favor ROS production in the reverse electron transfer mode.

In our model, electron flow is required for GB to induce ROS. Yet, GB cleavage of NDUFV1 might shorten the forward electron supply at a very early stage. One possibility to explain continuous electron flow and ROS production in this pathway is by the SC organization of the respiratory chain that allows reverse electron flow. GB treatment increases SC I+III_2 organization. In this setting, reverse flowing electrons might then leak at the level of damaged complex I to produce ROS. In addition, we cannot exclude that the effect of GB on other complexes, for example, complex II and III might also contribute to the ROS production. Mitochondrial cristae morphology also influences respiratory chain organization.[40,49] GB disrupts cristae junctions through an unknown mechanism, which likely contributes to mitochondrial dysfunction and ROS production.

Taken together, our results demonstrate that GB-induced respiratory chain complexes disruption triggers ROS production that is necessary for apoptosis.

Materials and Methods

Antibodies. Anti-V5 (V5-10) and anti-FLAG (M2) (Sigma-Aldrich, St. Louis, MO, USA); anti-PARP (H-250), anti-Hsp60 (H-300), anti-tubulin (B-7), anti-Tom40 and anti-HAX-1 (FL-279) (Santa Cruz Biotechnology, Dallas, TX, USA); anti-HA (3F10) (Roche Diagnostics (Schweiz AG), Rotkeuz, Switzerland); anti-κ-light-chain-HRP (Bethyl Laboratories, Inc., Montgomery, TX, USA); anti-NDUFS1 and anti-NDUFS2 (Epitomics, Abcam, Burlingame, CA, USA); anti-Tom20 and anti-Cyt *c* (BD Biosciences, San Jose, CA, USA); anti-NDUFV1 (Aviva Systems Biology, San Diego, CA, USA); anti-NDUFS3 (3F9DD2) (Invitrogen, Life Technologies, Grand Island, NY, USA); anti-NDUFS7 (Acris, Herford, Germany; AP21286PU-N); NDUFS13 (Mitosciences, Eugene, OR, USA; MS103); anti-CORE1/UQCRC1 (MS303), anti-CORE2/UQCRC2 (MS304) and anti-UQCRFS1 (MS305) (Abcam); anti-Endo G (Novus Biological, Littleton, CO, USA); anti-caspase-3 (3G2) and anti-histone H3 (Cell Signaling).

P and GB treatment. P was purified from the rat RNK-16 cells and GB from the human YT-Indy NK cells.[50] GB was first added to cells (5×10^4) suspended in 30 μl cell buffer (Hank's balanced salt solution (HBSS) with 10 mM HEPES, pH 7.4, 0.4% BSA, 4 mM $CaCl_2$) and immediately thereafter an equal volume of P in HBSS with 10 mM HEPES, pH 7.4, was added. The P concentration was chosen as the sublytic concentration that lyses 5–15% of cells. Cells were incubated at 37 °C for the indicated time. In some cases, cells were preincubated with 100 μM of the caspase inhibitors z-VAD-fmk+DEVD-fmk or 100 μM of the GB inhibitor Ac-IETD-CHO for 30 min at 37 °C before P and GB treatment. When antioxidants were used, cells were pretreated with *N*-acetyl-L-cysteine (Sigma-Aldrich) for 1 h or with MnTBAP (Calbiochem) for 30 min before the addition of P and GB. For the mitochondria-targeted antioxidant MitoQ, cells were preincubated for 1 h with 20 μM of MitoQ (kindly provided by Dr. Mike Murphy from the Mitochondrial Biology Unit, MRC UK, Cambridge, UK) or 20 μM of decyl-TPP (triphenylphosphonium) as a control, before treatment with P and GB.

Measurement of apoptosis, ROS production and ΔΨm. Treated cells were washed in PBS and stained with Annexin V Alexa Fluor-647 and PI (Life Technologies) to detect apoptotic cells. Alternatively, cells were fixed with 0.5% paraformaldehyde in PBS and nuclei were stained with 5 μg/ml Hoechst 33342 (Molecular Probes, Life Technologies) and analyzed by microscopy. Condensed or fragmented nuclei were considered as apoptotic. For each individual experiment, at least 300 nuclei were counted per condition. For detection of ROS, cells were stained with 5 μM MitoSOX or 2 μM HE (Life Technologies) for 5 min at room temperature (RT) and analyzed by flow cytometry. To assess ΔΨm, cells were labeled with 500 nM tetramethylrhodamine, methyl ester for 15 min at RT and washed three times in PBS before flow cytometry analysis with an Accuri C6 flow cytometer (BD Biosciences).

Site-directed mutagenesis. pCMV6 vectors containing NDUFS1, NDUFS2 and NDUFV1 cDNA sequences were purchased from OriGene Technologies (Rockville, MD, USA). Site-directed mutagenesis was performed by polymerase chain reaction with Herculase II Fusion DNA Polymerase (Agilent Technologies, Santa Clara, CA, USA) using overlapping primers, followed by restriction digest with *Dpn*I. PCR products were transformed into One Shot TOP10 Competent *Escherichia coli* (Life Technologies).

The following primers were used (5′–3′): S1D255A forward, GACAGAATCCATT GATGTAATGGCTGCGGTTGGAAG and S1D255A reverse, CTTCCAACCGCAGC CATTACATCAATGGATTCTGTC; S1D364A forward, GAGTGGACTCTGCCACCT TATGCACTGAAG and S1D364A reverse, CTTCAGTGCATAAGGTGGCAGAGTC CACTC; S2D317A forward, CGACCAGGTTGAGTTTGCTGTTCCTGTTGGTTCTC and S2D317A reverse, GAGAACCAACAGGAACAGCAAACTCAACCTGGTCG; and V1D118A forward, TGGTGAACGCAGCCGAGGGGGAGCC and V1D118A reverse, GGCTCCCCCTCGGCTGCGTTCACCA and V1D338/340A forward, CGGTGCTG ATGGCCTTCGCTGCGCTGGTGCA; V1D338/340A reverse, TGCACCAGCGCA GCGAAGGCCATCAGCACCG.

Generation of stable cell lines. Retroviral vectors were obtained by subcloning the cDNA sequence of human NDUFS1, NDUFS2 or NDUFV1 into pQCXIH, pQCXIP or pQCXIN (Takara, Clontech, Mountain View, CA, USA), respectively. The following primers were used (5′–3′): V1 forward, AAAAAATTAAT TAAGCCACCATGCTGGCAACACGGCGGC and V1 reverse (3xFLAG tag), forward, AAAAATTAATTAACTACTTGTCATCGTCATCCTTGTAGTCGATGTCATGATCTTTAT AATCACCGTCATGGTCTTTGTAGTCAGAGGCAGCCTGCCGGGC; S1, AAAAAAG CGGCCGCGCCACCATGTTAAGGATACCTGTAAGAAAG and S1 reverse (V5 tag), AAAAAAGGATCCTCACGTAGAATCGAGACCGAGGAGAGGGTTAGGGATAGGCTT ACCGCATATGGATGGTTCCTCTAC; S2 forward, AAAAAAGCGGCCGCGCCACCAT GGCGGCGCTGAGGGCTTTG and S2 reverse (HA tag), TGCTTCTGAATTCT CAAGCGTAGTCTGGGACGTCGTATGGGTACCGATCTACTTCTCCAAATACATATCTTGG.

Retroviruses were produced by $CaCl_2$ transfection of the GP2-293 packaging cell line with the retroviral vectors encoding complex I genes and pVSV-G. Twelve hours after transfection, cells were washed and stimulated with 10 mM sodium butyrate for 12 h before changing the medium. Retroviral supernatants were collected after 48 h. Cells were transduced by 12 h incubation with the retroviral supernatant in the presence of 8 μg/ml polybrene. Puromycin, G-418 and hygromycin selection was begun 48 h after infection.

Effector-target killing assay. Target cells (721.221, 0.05×10^6) in 100 μl of medium (HBSS containing 1.55 mM $CaCl_2$, 17.5 mM glucose, 10 mM HEPES, pH 7.4) were mixed with an equal volume of effector cells (YT-indy) at the indicated effector-to-target (E/T) ratios and incubated at 37 °C for the indicated times. The 5× loading buffer with β-mercaptoethanol was directly added to the mixture before SDS-PAGE and immunoblot. For caspase inhibition, target cells were pretreated for 15 min with 10 μM z-VAD-fmk before incubation with effector cells. For calcein release assay, target cells were preloaded with 10 μM Calcein AM (Life Technologies) for 30 min, then washed three times and incubated with effector cells as previously for the indicated time. Specific killing were determined by monitoring the calcein released in the supernatant:

$$\%\ \text{Specific release} = 100\frac{\text{release} - \text{spontaneous release}}{\text{max release} - \text{spontaneous release}}$$

Generation of ρ^0 cells. K562 cells were cultured in DMEM supplemented with ethidium bromide (250 ng/ml), sodium pyruvate (110 μg/ml) and uridine (50 μg/ml) for at least 1 month. Mitochondrial DNA was quantified by qPCR using primers specific for *COX1* and normalized to nuclear DNA using primers for *RNaseP*.

Cell fractionation. Treated cells (1×10^6) were washed with PBS and resuspended in 100 μl of cytosolic extraction buffer (70 mM KCl, 137 mM NaCl, 1.4 mM KH_2PO_4 pH 7.2, 4.3 mM Na_2HPO_4, 250 mM sucrose, 50 μg/ml D, protease inhibitors) and placed on ice for 5 min. Cells were centrifuged at 1000 × *g* for 5 min and the supernatant was stored as the cytosolic fraction. The pellet was resuspended in 100 μl of mitochondrial lysis buffer (50 mM Tris, pH 7.4, 150 mM NaCl, 2 mM EDTA, 2 mM EGTA, 2% Triton X-100, 0.3% NP-40, protease inhibitors). After 10 min of centrifugation at 10 000 × *g*, the supernatant was kept as the mitochondrial-enriched fraction.

Quantification of GB uptake. Cells were washed in HBSS and resuspended in cell buffer (HBSS with 10 mM HEPES, pH 7.4, 0.4% BSA, 4 mM $CaCl_2$). GB, labeled with Alexa Fluor-647 using the Alexa Fluor-647 Labeling Kit from Life Technologies according to the manufacturer's protocol, was added to cells just before adding a sublytic dose of P. After 10 min at 37 °C, cells were extensively washed with HBSS at 4 °C before flow cytometry analysis.

DNA laddering assay. Treated cells (1.5×10^6) were washed with cold PBS, resuspended in lysis buffer (10 mM Tris-HCl, pH 7.4, 10 mM EDTA, 0.5% SDS) and incubated for 10 min on ice. RNAse A (100 μg/ml) was added for 1 h at 37 °C, followed by the addition of 100 μg/ml PK for 4 h at 50 °C. After adding 300 mM sodium acetate, pH 5.2, DNA was precipitated with ethanol overnight at −20 °C. The pellet obtained after centrifugation at 14 000 × *g* for 30 min was dissolved in TE buffer (10 mM Tris, pH 8.0, 1 mM EDTA). DNA (6 μg) was electrophoresed through 1.2% agarose gels containing 0.5 μg/ml ethidium bromide.

Isolated mitochondria assays. Mitochondria isolated from mouse liver as described[51] were freshly prepared for all assays. Mitochondria (2.5 mg/ml protein) in 40 μl import buffer (600 mM sorbitol, 160 mM KCl, 20 mM magnesium acetate, 4 mM KH_2PO_4, 5 mM EDTA, 5 mM $MnCl_2$, 200 mM HEPES, pH 7.2) were incubated with GB (450 nM) for 5 min at 37 °C and 10 μl of reactions were analyzed by immunoblot. For apoptogenic factor release experiments, mitochondria were incubated with GB (450 nM) alone or with 25 μg of S100 for 1 h at 37 °C. After centrifugation at 8000 × *g*, supernatant and pellet were analyzed by immunoblot. For O_2 consumption and electron microscopy experiments, mitochondria were purified as described.[52] Mitochondrial pellet was resuspended in respiration buffer (150 mM KCl, 10 mM Tris/MOPS and 10 μM ATP). Mitochondria (400 μg) were transferred to a Clark electrode chamber to measure oxygen consumption. Succinate (5 mM) or glutamate and malate (5 and 2.5 mM, respectively) were added, and 5 min later GB (450 nM) was added. Oxygen consumption was recorded over 20 min. Mitochondrial import assays were performed according to Mokranjac and Neupert.[53] Fifty micrograms of mitochondria in the import buffer were incubated with 200 ng of unlabeled or Alexa-647 GB for 15 min at 37 °C. Half of the reactions were treated with 50 μg/ml of PK for 15 min on ice to give the imported fraction. PK was inactivated with 5 μl of 0.2 M PMSF and sample spun at 12 000 × *g* for 15 min. Pellets were resuspended in either PBS or 1x SDS sample buffer for FACS and WB analysis, respectively. The second halves ware use as input. In some cases, mitochondria in SH buffer were preincubated with 0.4 μM of valinomycin for 15 min to disrupt the $\Delta\Psi$ before carrying the import assay.

Respiratory complex in-gel activity. Mitochondria (400 μg in 40 μl of import buffer) were treated with 450 nM of GB for 5 min at 37 °C. The reaction was stopped by adding 3 μl of 0.2 M PMSF. After 5 min on ice, samples were spun for 30 min at 12 000 × *g*. Pellets were solubilized on ice for 15 min with 40 μl of lysis buffer. For monomeric complex resolution, pellets were resuspended in LM buffer (50 mM NaCl, 1 mM EDTA, 50 mM imidazole/HCl, 2 mM 6-aminohexanoic acid, pH 7.0, 2% freshly prepared LM). To resolve SCs, pellets were solubilized in D buffer (30 mM HEPES, pH 7.4, 150 mM potassium acetate, 10% glycerol and 5% freshly prepared D). Samples were spun for 20 min at 20 000 × *g* at 4 °C. Six microliters of 50% glycerol and 5 μl of 5% Coomassie blue G-250 were added to the supernatant to give a detergent/dye mass ratio of 8. Mitochondria (100 μg) were electrophoresed at 30 V for 30 min through native 3–13% gradient acrylamide gels using anode buffer (imidazole 25 mM, pH 7) and cathode buffer B (50 mM Tricine, pH 7, 7.5 mM imidazole, 0.02% Coomassie blue G-250). Then, the cathode buffer B was replaced by cathode buffer A (50 mM Tricine, pH 7.0, 7.5 mM imidazole, 0.002% Coomassie blue G-250) and electrophoresis was continued at 80 V until the dye front reached the gel bottom. Complex I, IV and V were assayed as described.[38] Briefly, gels were washed in distilled water before incubation at RT with the following solutions: Complex I solution – 2 mM Tris-HCl, pH 7.4, 0.1 mg/ml NADH, 2.5 mg/ml nitrotetrazolium blue for 15 min at RT. Complex IV solution – 5 mg 3:3′-diamidobenzidine tetrahydrochloride dissolved in 9 ml of 5 mM phosphate buffer (0.05 M, pH 7.4), 1 nM catalase (20 U/ml), 10 mg Cyt *c* and 750 mg sucrose overnight at RT. Complex V solution – 35 mM Tris, pH 7.8, 270 mM glycine, 14 mM $MgSO_4$, 0.2% $Pb(NO_3)_2$, 8 mM ATP and overnight at RT. Gels were washed in distilled water and scanned immediately. Complex III activity was assayed as described in Smet *et al.*[39] Briefly, gels were incubated in Complex III solution – 1-STEP TMB-BLOT (Pierce, Thermo Scientific, Rockford, IL, USA) overnight at RT.

Spectrophotometric respiratory complex assay. Mitochondria (60 μg in 30 μl of import buffer) were treated with 450 nM of GB for 5 min at 37 °C. The reaction was stopped by adding 3 μl of 0.2 M PMSF. After 5 min on ice, the respiratory complex activities were measured according to Spinazzi *et al.*[54]

For complex I, the activity samples were subjected to three freeze–thraw cycles before assays.

Seahorse oxygen consumption. K562 and its ρ^0 cells were plated overnight at a density of 40 000 cells per well in unbuffered assay medium supplemented with 25 mM glucose, 1 mM pyruvate, 4 mM glutamine (same as their culture medium). One hour before measurement, medium was replaced for unbuffered assay medium at 37 °C without CO_2. Centrifugation of the plate at 1200 r.p.m. for 15 min allows suspension cells to attach for this assay. Measurement of intact cellular respiration was performed using the Seahorse XF24 analyzer (Seahorse Bioscience, North Billerica, MA, USA). Respiration was measured under basal condition, and in the presence of 1 μM ATP synthase inhibitor oligomycin, 0.75 μM uncoupler FCCP, 1 μM mitochondrial respiration complex I inhibitor Rotenone and 1 μM mitochondrial respiration complex III inhibitor antimycin A.

Blue native-PAGE immunoblot. Mitochondria (10 μg), resolved by BNGE as above, were transferred onto PVDF membranes using a semidry Hoefer transfer apparatus. Membranes were fixed in 100% methanol before blocking and incubation at 4 °C overnight with primary antibodies.

Electron microscopy. Mouse liver mitochondria (400 μg) in 40 μl import buffer were treated with 450 nM GB with or without 25 μg S100 for 1 h at 37 °C. Samples were washed two times in 1 × PBS and then fixed for 30 min at RT with 1.25% glutaraldehyde and 100 mM sodium cacodylate. Embedding and staining were performed as in Scorrano *et al.*[55] Thin sections were imaged on a Tecnai-20 electron microscope (Technai 20 FEI Company, Eindhoven, Netherlands). The number of mitochondria with disrupted cristae junctions was counted in 1200 mitochondria for each condition.

Conflict of Interest

The authors declare no conflict of interest.

Acknowledgements. This work was supported by Ambizione SNSF PZ00P3_126710/1, ERC starting Grant ERC-2010-StG_20091118 and subsides from the Carlos and Elsie de Reuter Foundation and Schmidheiny Foundation. We thank Prof. Krause for NOX1$^{-/-}$ and NOX4$^{-/-}$ embryos (University of Geneva, Geneva, Switzerland) and Olivier Dupont for technical assistance.

1. Chowdhury D, Lieberman J. Death by a thousand cuts: granzyme pathways of programmed cell death. *Annu Rev Immunol* 2008; **26**: 389–420.
2. Cullen SP, Adrain C, Luthi AU, Duriez PJ, Martin SJ. Human and murine granzyme B exhibit divergent substrate preferences. *J Cell Biol* 2007; **176**: 435–444.
3. Andrade F, Roy S, Nicholson D, Thornberry N, Rosen A, Casciola-Rosen L. Granzyme B directly and efficiently cleaves several downstream caspase substrates: implications for CTL-induced apoptosis. *Immunity* 1998; **8**: 451–460.
4. Kroemer G, Galluzzi L, Brenner C. Mitochondrial membrane permeabilization in cell death. *Physiol Rev* 2007; **87**: 99–163.
5. MacDonald G, Shi L, Vande Velde C, Lieberman J, Greenberg AH. Mitochondria-dependent and -independent regulation of Granzyme B-induced apoptosis. *J Exp Med* 1999; **189**: 131–144.
6. Sutton VR, Wowk ME, Cancilla M, Trapani JA. Caspase activation by granzyme B is indirect, and caspase autoprocessing requires the release of proapoptotic mitochondrial factors. *Immunity* 2003; **18**: 319–329.
7. Waterhouse NJ, Sedelies KA, Browne KA, Wowk ME, Newbold A, Sutton VR *et al.* A central role for Bid in granzyme B-induced apoptosis. *J Biol Chem* 2005; **280**: 4476–4482.
8. Goping IS, Barry M, Liston P, Sawchuk T, Constantinescu G, Michalak KM *et al.* Granzyme B-induced apoptosis requires both direct caspase activation and relief of caspase inhibition. *Immunity* 2003; **18**: 355–365.
9. Alimonti JB, Shi L, Baijal PK, Greenberg AH. Granzyme B induces BID-mediated cytochrome *c* release and mitochondrial permeability transition. *J Biol Chem* 2001; **276**: 6974–6982.
10. Kaiserman D, Bird CH, Sun J, Matthews A, Ung K, Whisstock JC *et al.* The major human and mouse granzymes are structurally and functionally divergent. *J Cell Biol* 2006; **175**: 619–630.
11. Han J, Goldstein LA, Hou W, Froelich CJ, Watkins SC, Rabinowich H. Deregulation of mitochondrial membrane potential by mitochondrial insertion of granzyme B and direct Hax-1 cleavage. *J Biol Chem* 2010; **285**: 22461–22472.
12. Heibein JA, Barry M, Motyka B, Bleackley RC. Granzyme B-induced loss of mitochondrial inner membrane potential (Delta Psi m) and cytochrome *c* release are caspase independent. *J Immunol* 1999; **163**: 4683–4693.
13. Thomas DA, Scorrano L, Putcha GV, Korsmeyer SJ, Ley TJ. Granzyme B can cause mitochondrial depolarization and cell death in the absence of BID, BAX, and BAK. *Proc Natl Acad Sci USA* 2001; **98**: 14985–14990.
14. Balsa E, Marco R, Perales-Clemente E, Szklarczyk R, Calvo E, Landázuri MO *et al.* NDUFA4 is a subunit of complex IV of the mammalian electron transport chain. *Cell Metab* 2012; **16**: 378–386.
15. Ricci JE, Muñoz-Pinedo C, Fitzgerald P, Bailly-Maitre B, Perkins GA, Yadava N *et al.* Disruption of mitochondrial function during apoptosis is mediated by caspase cleavage of the p75 subunit of complex I of the electron transport chain. *Cell* 2004; **117**: 773–786.
16. Martinvalet D, Dykxhoorn DM, Ferrini R, Lieberman J. Granzyme A cleaves a mitochondrial complex I protein to initiate caspase-independent cell death. *Cell* 2008; **133**: 681–692.
17. Martinvalet D, Zhu P, Lieberman J. Granzyme A induces caspase-independent mitochondrial damage, a required first step for apoptosis. *Immunity* 2005; **22**: 355–370.
18. Beresford PJ, Xia Z, Greenberg AH, Lieberman J. Granzyme A loading induces rapid cytolysis and a novel form of DNA damage independently of caspase activation. *Immunity* 1999; **10**: 585–594.
19. Fan Z, Beresford PJ, Oh DY, Zhang D, Lieberman J. Tumor suppressor NM23-H1 is a granzyme A-activated DNase during CTL-mediated apoptosis, and the nucleosome assembly protein SET is its inhibitor. *Cell* 2003; **112**: 659–672.
20. Martinvalet D, Thiery J. A novel caspase-independent apoptotic pathway triggered by ganzyme A]. *Med Sci (Paris)* 2008; **24**: 901–903.
21. Kelso GF, Porteous CM, Coulter CV, Hughes G, Porteous WK, Ledgerwood EC *et al.* Selective targeting of a redox-active ubiquinone to mitochondria within cells: antioxidant and antiapoptotic properties. *J Biol Chem* 2001; **276**: 4588–4596.
22. Sherwood S, Hirst J. Investigation of the mechanism of proton translocation by NADH: ubiquinone oxidoreductase (complex I) from bovine heart mitochondria: does the enzyme operate by a Q-cycle mechanism? *Biochem J* 2006; **400**: 541–550.
23. Ngu LH, Nijtmans LG, Distelmaier F, Venselaar H, van Emst-de Vries SE, van den Brand MA *et al.* A catalytic defect in mitochondrial respiratory chain complex I due to a mutation in NDUFS2 in a patient with Leigh syndrome. *Biochim Biophys Acta* 2012; **1822**: 168–175.
24. Pagniez-Mammeri H, Loublier S, Legrand A, Bénit P, Rustin P, Slama A. Mitochondrial complex I deficiency of nuclear origin I. Structural genes. *Mol Genet Metab* 2012; **105**: 163–172.
25. Pagniez-Mammeri H, Rak M, Legrand A, Bénit P, Rustin P, Slama A. Mitochondrial complex I deficiency of nuclear origin II. Non-structural genes. *Mol Genet Metab* 2012; **105**: 173–179.
26. Hirst J, Carroll J, Fearnley IM, Shannon RJ, Walker JE. The nuclear encoded subunits of complex I from bovine heart mitochondria. *Biochim Biophys Acta* 2003; **1604**: 135–150.
27. Igarashi Y, Eroshkin A, Gramatikova S, Gramatikoff K, Zhang Y, Smith JW *et al.* CutDB: a proteolytic event database. *Nucleic Acids Res* 2007; **35**: D546–D549.
28. Lapuente-Brun E, Moreno-Loshuertos R, Acín-Pérez R, Latorre-Pellicer A, Colás C, Balsa E *et al.* Supercomplex assembly determines electron flux in the mitochondrial electron transport chain. *Science* 2013; **340**: 1567–1570.
29. Lazarou M, McKenzie M, Ohtake A, Thorburn DR, Ryan MT. Analysis of the assembly profiles for mitochondrial- and nuclear-DNA-encoded subunits into complex I. *Mol Cell Biol* 2007; **27**: 4228–4237.
30. McKenzie M, Ryan MT. Assembly factors of human mitochondrial complex I and their defects in disease. *IUBMB Life* 2010; **62**: 497–502.
31. Wei MC, Zong WX, Cheng EH, Lindsten T, Panoutsakopoulou V, Ross AJ *et al.* Proapoptotic BAX and BAK: a requisite gateway to mitochondrial dysfunction and death. *Science* 2001; **292**: 727–730.
32. Petrosillo G, Ruggiero FM, Paradies G. Role of reactive oxygen species and cardiolipin in the release of cytochrome *c* from mitochondria. *FASEB J* 2003; **17**: 2202–2208.
33. Petrosillo G, Ruggiero FM, Pistolese M, Paradies G. Ca^{2+}-induced reactive oxygen species production promotes cytochrome c release from rat liver mitochondria via mitochondrial permeability transition (MPT)-dependent and MPT-independent mechanisms: role of cardiolipin. *J Biol Chem* 2004; **279**: 53103–53108.
34. Kim JS, Lee JH, Jeong WW, Choi DH, Cha HJ, Kim do H *et al.* Reactive oxygen species-dependent EndoG release mediates cisplatin-induced caspase-independent apoptosis in human head and neck squamous carcinoma cells. *Int J Cancer* 2008; **122**: 672–680.
35. Huai J, Vögtle FN, Jöckel L, Li Y, Kiefer T, Ricci JE *et al.* TNFalpha-induced lysosomal membrane permeability is downstream of MOMP and triggered by caspase-mediated NDUFS1 cleavage and ROS formation. *J Cell Sci* 2013; **126**: 4015–4025.
36. Aguilo JI, Anel A, Catalán E, Sebastián A, Acín-Pérez R, Naval J *et al.* Granzyme B of cytotoxic T cells induces extramitochondrial reactive oxygen species production via caspase-dependent NADPH oxidase activation. *Immunol Cell Biol.* 2010; **88**: 545–554.
37. Kaminski M, Kiessling M, Suss D, Krammer PH, Gulow K. Novel role for mitochondria: protein kinase Ctheta-dependent oxidative signaling organelles in activation-induced T-cell death. *Mol Cell Biol* 2007; **27**: 3625–3639.
38. Nijtmans LG, Henderson NS, Holt IJ. Blue Native electrophoresis to study mitochondrial and other protein complexes. *Methods* 2002; **26**: 327–334.
39. Smet J, De Paepe B, Seneca S, Lissens W, Kotarsky H, De Meirleir L *et al.* Complex III staining in blue native polyacrylamide gels. *J Inherit Metab Dis.* 2011; **34**: 741–747.

40. Cogliati S, Frezza C, Soriano ME, Varanita T, Quintana-Cabrera R, Corrado M *et al.* Mitochondrial cristae shape determines respiratory chain supercomplexes assembly and respiratory efficiency. *Cell* 2013; **155**: 160–171.
41. Murphy MP. How mitochondria produce reactive oxygen species. *Biochem J* 2009; **417**: 1–13.
42. Malassagne B, Ferret PJ, Hammoud R, Tulliez M, Bedda S, Trébéden H *et al.* The superoxide dismutase mimetic MnTBAP prevents Fas-induced acute liver failure in the mouse. *Gastroenterology* 2001; **121**: 1451–1459.
43. Walch M, Dotiwala F, Mulik S, Thiery J, Kirchhausen T, Clayberger C *et al.* Cytotoxic cells kill intracellular bacteria through granulysin-mediated delivery of granzymes. *Cell* 2014; **157**: 1309–1323.
44. Sazanov LA, Hinchliffe P. Structure of the hydrophilic domain of respiratory complex I from *Thermus thermophilus. Science* 2006; **311**: 1430–1436.
45. Dudkina NV, Eubel H, Keegstra W, Boekema EJ, Braun HP. Structure of a mitochondrial supercomplex formed by respiratory-chain complexes I and III. *Proc Natl Acad Sci USA* 2005; **102**: 3225–3229.
46. Dudkina NV, Kouril R, Peters K, Braun HP, Boekema EJ. Structure and function of mitochondrial supercomplexes. *Biochim Biophys Acta* 2010; **1797**: 664–670.
47. Lambert AJ, Brand MD. Inhibitors of the quinone-binding site allow rapid superoxide production from mitochondrial NADH:ubiquinone oxidoreductase (complex I). *J Biol Chem* 2004; **279**: 39414–39420.
48. Lambert AJ, Brand MD. Superoxide production by NADH:ubiquinone oxidoreductase (complex I) depends on the pH gradient across the mitochondrial inner membrane. *Biochem J* 2004; **382**: 511–517.
49. Frezza C, Cipolat S, Martins de Brito O, Micaroni M, Beznoussenko GV, Rudka T *et al.* OPA1 controls apoptotic cristae remodeling independently from mitochondrial fusion. *Cell* 2006; **126**: 177–189.
50. Thiery J, Walch M, Jensen DK, Martinvalet D, Lieberman J. Isolation of cytotoxic T cell and NK granules and purification of their effector proteins. *Curr Protoc Cell Biol* 2010; (Chapter 3, Unit 3) 37.
51. Susin SA, Larochette N, Geuskens M, Kroemer G. Purification of mitochondria for apoptosis assays. *Methods Enzymol* 2000; **322**: 205–208.
52. Frezza C, Cipolat S, Scorrano L. Organelle isolation: functional mitochondria from mouse liver, muscle and cultured fibroblasts. *Nat Protoc* 2007; **2**: 287–295.
53. Mokranjac D, Neupert W. Protein import into isolated mitochondria. *Methods Mol Biol* 2007; **372**: 277–286.
54. Spinazzi M, Casarin A, Pertegato V, Salviati L, Angelini C. Assessment of mitochondrial respiratory chain enzymatic activities on tissues and cultured cells. *Nat Protoc* 2012; **7**: 1235–1246.
55. Scorrano L, Ashiya M, Buttle K, Weiler S, Oakes SA, Mannella CA *et al.* A distinct pathway remodels mitochondrial cristae and mobilizes cytochrome *c* during apoptosis. *Dev Cell* 2002; **2**: 55–67.

Supplementary Information accompanies this paper on Cell Death and Differentiation website (http://www.nature.com/cdd)